The 2017 World Congress on
Advances in Structural Engineering and Mechanics (ASEM17)
28 August - 1 September, 2017, Ilsan(Seoul), Korea

Reduce the Noise Emission of Railroad Freight Cars by a New Method Using Evolutionary Optimisation Strategy

Entuo Liu[1)] and *Manfred W. Zehn[2)]

[1),2)]*Structural and Computational Mechanics, Institute of Mechanics, Technische Universität (TU) Berlin, 10623 Berlin, Germany*

ABSTRACT

The change of transport technology in Europe has seen many railroad freight cars returning empty after unloading. Some of those wagons have been in service unchanged for many years now and the bodies of the empty wagons in operation remarkably contribute to total radiation of noise. For the necessary acceptance of more rail traffic for environmental reasons it is essential to develop innovative freight wagons or change existing ones with lower noise emission. Since panels and other areas with thin walled parts of the freight cars are much more prone to noise radiation than other components. It is therefore advisable to improve their acoustic behaviour. For that purpose, a new structural optimization methodology has been developed and employed. It will be presented in this paper, based on the optimisation of a curvilinear stiffener and point masses attached to the surface of the panels. The Covariance Matrix Adaptation Evolution Strategy (CMA-ES) optimisation strategy is adopted to find out optimal combination of the stiffener (and its shape) and masses within a FE model with automatically adaption of the FE mesh during optimisation. The new methodology is exemplified in the minimization of the sound power radiated from the surface of a simply supported rectangular plate. But it has been also extended to a panel of a real freight car using a sub-model method in ABAQUS. The method has proved to be effective in reducing the power radiated from the panel in a given frequency range with complex boundary condition. The total mass only insignificantly increases compared to the whole wagon. The method is very useful to improve the acoustic behaviour of existing wagons or for new innovative designs to be developed. It can be applied to curved panels to reduce noise, e.g. tank wagons, as well. It is also cost-effective since the attached components are made of steel or the same material as the surface and they are easy to manufacture and mount as well.

[1)]Dr.-Ing.
[2)]Professor

1. Introduction

Rail freight saves considerable carbon dioxide emission compared to road transport due to its intrinsic energy-efficient nature. Rail transport has also a reliability advantage due to a strict operational timetable. However, according to the report [1], a considerable number of empty runs of goods waggons are unavoidable, but unloaded waggons produce more noise emissions than loaded ones. Such burdens can only be partially compensated for by erecting noise barriers. As a consequence, it is necessary to reduce the noise emission from empty running freight cars. Since panels and other areas with thin walled parts of the freight cars are much more prone to noise radiation than other components, it is therefore advisable to improve their acoustic behaviour. Many methods have been studied to generate panels with weaker noise radiation. For example, Pierre and Koopman [2] attached discrete point masses to the surface of the panel in order to reduce the power at resonances. Rousounelos [3] attached straight stiffeners and point masses to panels to study their properties with regard to acoustic radiation. Banerjee [4] studied the application of piezo fibre composite patches with interdigitated electrodes as actuators to maximally reduce the sound power from a plate. Toyoda and Takahashi [5] relate the sound radiation to the impedance and tried to reduce the radiated power by controlling the impedance. Although, it is very common to use point masses [6-8] and/or straight stiffeners [3] to reduce the sound emission from panels, a combination of employing point masses and curved stiffeners has rarely been studied to change acoustic responses. In this paper, an approach with curved stiffener and/or point masses will be presented to minimize the sound power radiated from a rectangular panel. The well-known global optimization algorithm CMA-ES has been adopted to obtain the optimum of the design variables. Compared to the deployment of straight stiffeners and/or point masses, this method has found to be very promising, because the shape of a curvilinear stiffener is flexible to adapt on the surface of the panels. This method is helpful to reduce noise from the current wagons in market and also can be adopted to develop new innovative wagons.

2. FEM of Plate Attaching Curvilinear Stiffener and/or Point Masses

This section outlines the technique to model a plate with a curvilinear stiffener and/or point masses attached as shown in Fig. 1. The plate in this example is simply supported and excited by a force perpendicular to the surface. One curvilinear stiffener and/or one or more point masses (m1, m2, …) can be attached to the plate. In order to reduce the computational effort during optimisation, the plate is meshed only once in the beginning of optimisation while the stiffener and the point masses positions are always automatically meshed in each step.

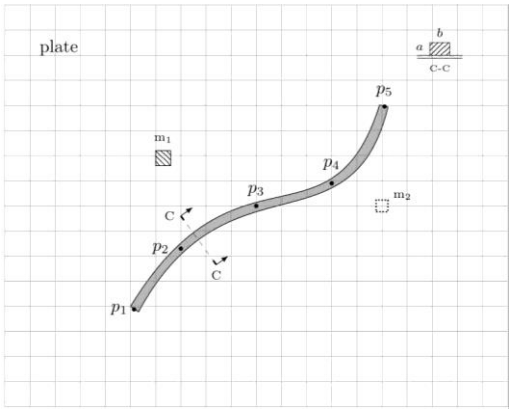

Figure 1: A Plate Carrying Stiffener and Point Masses

Therefore, they must be connected to the plate by constraint. That enables that during structural optimisation the point masses and the stiffener can change positions arbitrarily on the surface of the plate. This approach has the other advantage that it makes it much easier to calculate the sound radiation by numerical method.

2.1 Plate with Attached Point Masses

More than one point mass can be attached to the plate. In this paper, the inertia properties and shape of the mass are not considered and therefore they are assumed to be point masses. The position of point mass is randomly changed during optimisation. When the calculated position of a point mass does not coincide with nodes of the shell elements modelling the plate, it will be connected to the shell element by a mass distribution approach as shown in Fig. 2.

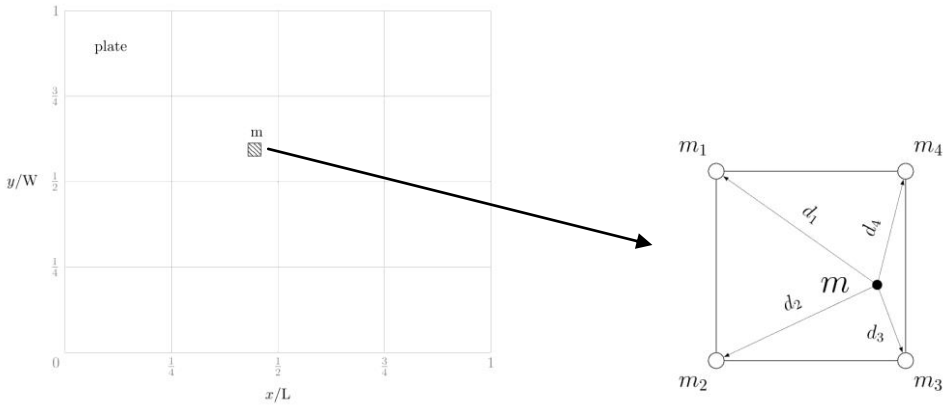

Figure 2: Distribution of Mass to Nodes of the Shell Element

The point mass m is located inside of a shell element. The distances between m and the nodes of one shell element are $d_i(i=1,2,3,4)$. m is divided into four parts $m_i(i=1,2,3,4)$ according to the distances $d_i(i=1,2,3,4)$ through

$$\frac{m_i}{m}=1-\frac{d_i}{\sum d_i}(i=1,2,3,4) \tag{1}$$

Each m_i is then automatically coupled to the corresponding node of the shell element. As seen in Eq. 1, the smaller the distance d_i is, the larger mass is distributed to a node. The mass-distribution method is easy to operate in an FEM system (e.g. ABAQUS) and induces only a small error. When comparing eigenfrequencies of the plate with attached point masses, using direct node-coupling method as reference, the maximal relative error of the first ten modes, caused by the mass-distribution method, is smaller than 1.0%. This approach has little influence from the additional mass as shown in Fig. 3 (left). When the control element size is the same (e.g. 25mm), the maximal error is no greater than 0.5% as the mass increases from 0.3kg to 0.8kg with steps of 0.1kg. It is also independent of the shell element size as shown in Fig. 3 (right). If the mass is fixed (e.g. 0.613kg), the maximal error is round about 1.0% as the shell element size increases from 15mm to 50mm. In general, the error of each eigenfrequency decreases for a finer mesh. Therefore, the error induced by the mass-distribution method can be neglected during the optimisation.

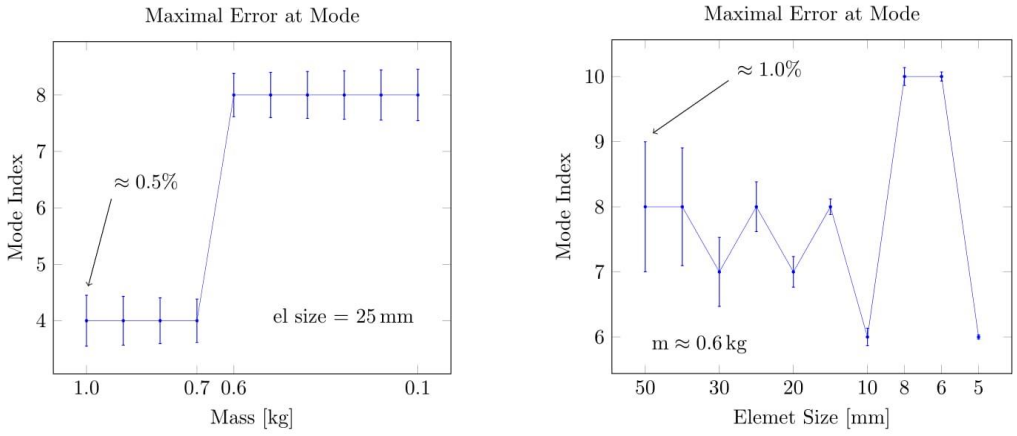

Figure 3: Maximum of Relative Error at Modes

2.2 Plate with Mounted Curved Stiffener

The cross section of the stiffener is assumed to be rectangular and its dimension does not change during optimisation. The stiffener is connected to one surface of the plate by defining the distance from its centre to the neutral surface of plate. The stiffener is modelled with linear beam elements. All the nodes along the stiffener are connected to the plate by multi-point constraints (MPC) as shown in Fig. 4.

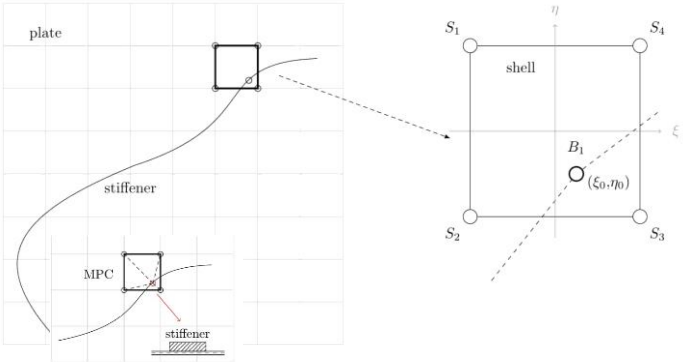

Figure 4: Connection of Stiffener and Plate

Every node along the stiffener is connected to 4 nodes of one shell element by linear MPC. As shown in Fig. 3, if one node B_1 on the stiffener is located within one shell element, B_1 is then connected to nodes $S_i(i=1,2,3,4)$ through MPC. Therefore, the following equation holds:

$$Nu_i^T = u_i^{B_1}(i=1,2,...,6) \tag{2}$$

where i is the index of degree of freedom (DOF), $u_i = \left[u_i^{S_1}, u_i^{S_2}, u_i^{S_3}, u_i^{S_4}\right]^T$ and $N = \left[N_1, N_2, N_3, N_4\right]^T$ is the vector of shape functions for the shell element at coordinate (ξ_0, η_0) as shown in Fig. 3. Note, that all the nodes from beam elements are selected as slave nodes to avoid a false chain constraint. As seen in Eq. 2, the DOF index on both sides of the equation is the same. This means that the cross influence between constraints is not taken into consideration and each constraint (i) is independent to the others ($j \neq i$). Such a constraint condition can reduce the total number of DOFs and therefore save much computational effort. It also has the benefit of easily generating the constraints in the programed algorithm. The error induced from Eq. 2 can be studied by comparing the eigenfrequencies of a plate with attached stiffener using direct a node coupling method. As shown in Fig. 5, for example, the stiffener (left) is connected to the plate by MPC while the stiffener (right) is automatically coupled to the plate along the sharing nodes. The influence induced by mixed-elements from the model (right) can be neglected since the number of triangular elements is very small and all elements are well regularly meshed.

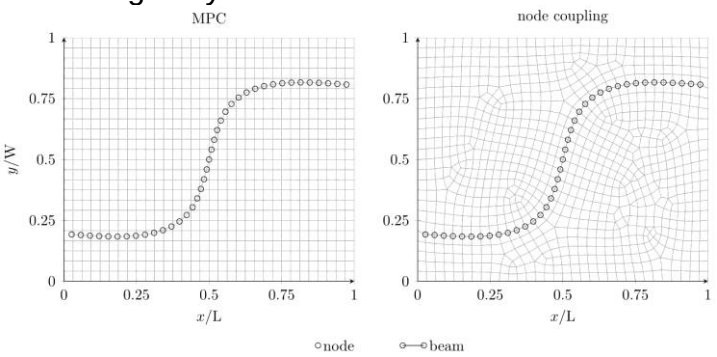

Figure 5: Plate with the Stiffener attached by MPC and Automatic Node Coupling

The eigenfrequencies obtained from the plate using node-coupling method are assumed as references. The characteristic size of elements is selected to be 10mm, 15mm, 20mm, 30mm, 40mm or 50mm and both of the FE models are generated based upon one of the element size.

The results show that the maximal error is smaller than 5%, which occurs for element size 50mm. The relative error of the first ten eigenfrequencies increases as the characteristic element size becomes larger. In addition, the number of constrained DOFs has influence to the results as well. If only the DOFs 1, 2 and 3 are constraint, the maximal error is round about 4.2%. Whereas if the DOFs 1 to 4 are constraint, the overall error at each eigenfrequency can be further reduced, but additional constraints of the 5th

and 6th DOFs do not have much influence. Therefore, it can be concluded that the error from the MPC is very small and can be neglected during the optimisation.

3. Radiated Sound Power Formulation

The sound power radiated from a plate can be obtained by the well-known Rayleigh integral.

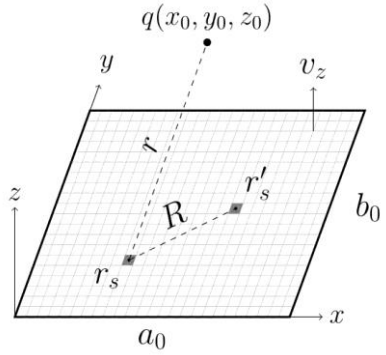

Figure 6: Plate with Infinite Rigid Baffle

As shown in Fig. 6, the plate is imbedded in an infinite rigid baffle and vibrates out of plane. The total sound power P radiated from the surface is according to [2]

$$P = \frac{1}{2}\iint v(r_s)\frac{\omega\rho}{2\pi}\frac{\sin(k_0 R)}{R}v^*(r_S')dSdS' \tag{3}$$

where r_s and r_s' are two evaluating points on surface, ρ is the fluid density, v is complex and indicates the velocity in the direction of z, v^* indicates complex conjugate, R is the distance between r_s and r_S', $k_0(=\omega/c)$ is the wave number, and $S\,(a_0 \times b_0)$ indicates the area of the surface. Note that $S'(=S)$ is used only to indicate a double integral. The singularity in Eq. 3 is already released since $^{\sin(k_0 R)}/_{k_0 R} \to 0$, when $R \to 0$.

When the surface is meshed into finite rectangular shell elements, P can be approximated using one Gaussian point integral

$$P \approx \frac{k_0\omega\rho}{4\pi}\sum_{i=1}^{n}\sum_{j=1}^{n} v_i \frac{\sin(k_0 R_{ij})}{k_0 R_{ij}} v_j^* e_i e_j \tag{4}$$

where v_i and v_j^* (* indicates the complex conjugate) are the velocity at the centre of element i and j, e_i and e_j indicate the element areas, R_{ij} is the distance between the centres of element i and j, and n is the total number of elements. Eq. 4 can be used to approximate the power radiation from the surface. The results using one Gaussian point are 5% in error compared with the integral using 4 or more Gaussian points [9]. In addition, the largest element size is much smaller compared with the acoustic wavelength in the frequency range of interest throughout this paper. The con-

tribution from neighbouring modes is already considered, which means that Eq. 4 can approximately evaluate the power in high frequency range with high modal density [2].

4. Optimization Formulation

CMA-ES is the abbreviation of Covariance Matrix Adaptation Evolutionary Strategy. It has been integrated into the FEM system, for the investigations of the authors, to find the global optimum. The CMA-ES is a stochastic numerical method and it is best suitable for non-linear or non-convex continuous optimization problems [10]. It is a good choice for problems in which the object function has no specific formulations. For more details on this subject see for example [11, 12].

In low frequency range the modal density is lower and it is assumed that the sound power radiated at a resonance is dominated by the contribution at resonances. For a low damped model the total sound power within a frequency band can be approximated by summing up the powers from all resonances in the band. However, the lowest or the highest resonance in this band may probably run out of the band during structure optimization. In order to keep the total number of resonances within a frequency band, the object function $f(\bar{x})$ can be defined as the power radiated from a number of resonances

$$f(\bar{x}) = \sum_{i=1}^{N} P_i (i = 1,2,...,\pi) \tag{5}$$

where N is the total number of resonances, P_i is the power at the i th resonance, and $\bar{x}$ is a vector describing the placement (and mass) of the stiffener and point masses. The index i can be selected continuously or discontinuously. For example, i can be selected as $i = 1,2,3$ or $i = 1,4,6,9$. The unit of P is Watt instead of decibel during the structural optimisation. Note that the resonances are changing during the structural optimisation. The distance of resonance floating depends on the mode (i) under optimisation, the stiffener, and the point masses. As it is of primary importance to study the power at resonances, the influence of frequency floating is not considered further in this paper.

The developed and programmed CMA-ES algorithm runs as a PYTHON script in ABAQUS. The flowchart of the optimisation is shown in Fig. 7.

5. Special Considerations during the Optimisation

Special considerations must be taken into account and carefully managed, when the structural optimisation problem is integrated within the CMA. Otherwise, the CMA cannot find successfully the global minimum or collapses suddenly due to numerical errors. Therefore, the following two problems regarding the scaling of point masses and shape control of curved stiffeners are studied particularly.

5.1 Scaling of Mass

Each point mass is described by parameters of placement and mass

$$x_{m1}, y_{m1}, ..., m_1, ...$$

where m_1 indicates the mass of the first point mass. The masses (m_1,⋯) usually do not have the same magnitude as the coordinates (x_{m1}, y_{m1},⋯). The difference of magnitude increases the numerical error during the optimisation and may probably make the

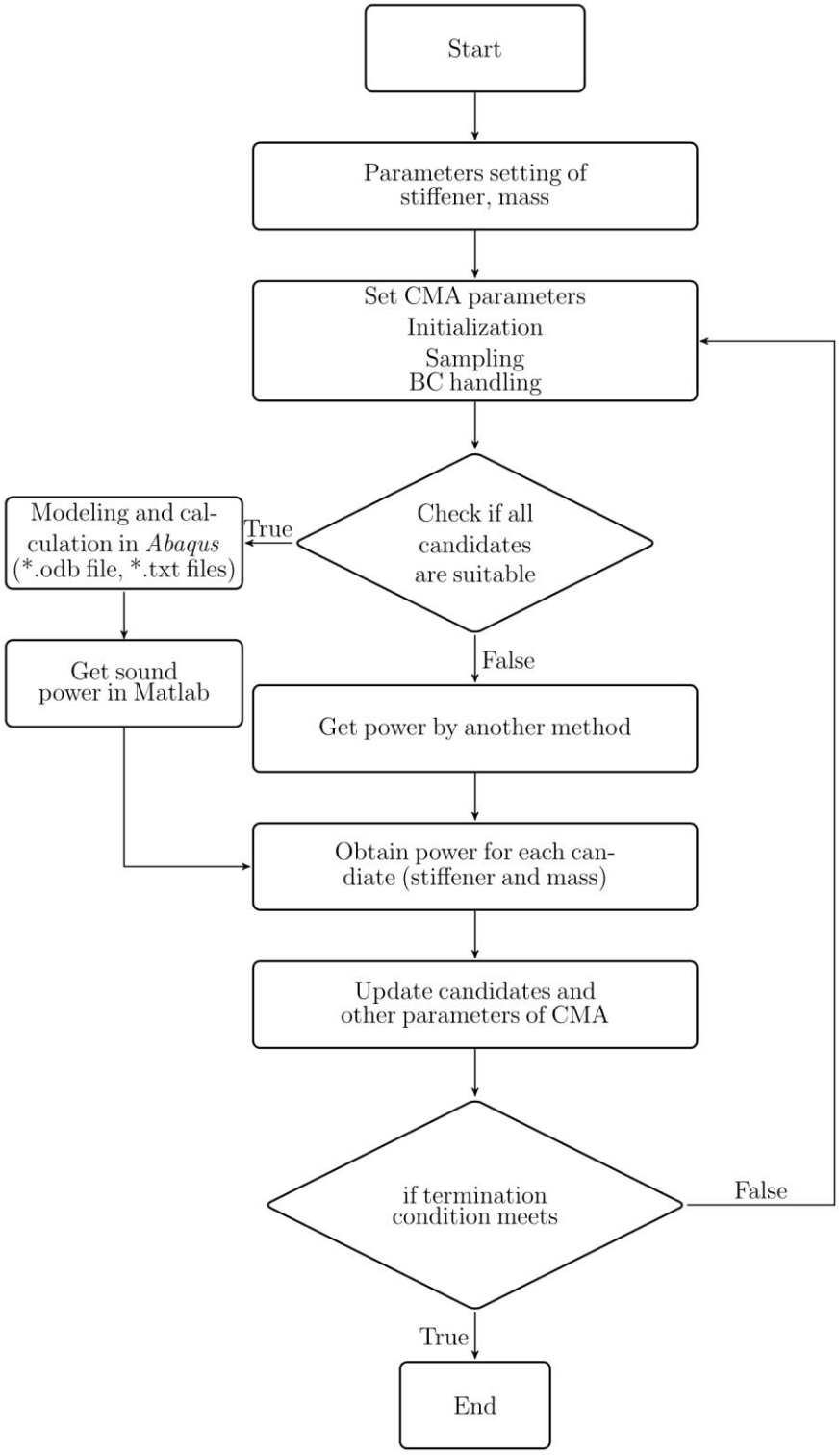

Figure 7: Flowchart of the Optimisation Process

optimisation process not convergent to the global minimum. To overcome this problem, a scaling factor w_0 has been introduced. The masses (m_1,⋯) are multiplied by to adjust the magnitude towards coordinates. Note that the scaling factor w_0 must be get rid of during the FEM is calculation in ABAQUS to obtain the sound power.

5.2 Shape Control of the Stiffener

The shape of a curved stiffener in this paper is described by a spline function in ABAQUS. It is controlled by 5 points

$$x_1, y_1, ..., x_5, y_5$$

It is believed that the shape takes advantage from the symmetry in the dynamic responses. Therefore, the stiffener is set symmetrically about the centre of the plate by fixing the third point (x_3, y_3). The symmetry of the shape has also the other advantage of reducing particularly the computational effort.

The coordinates of the spline arbitrarily change within the surface of the plate. Probably, stiffeners will appear, which cannot be calculated in ABAQUS due to its intrinsic limitation. In order to make the optimisation process run continuously, the following defective shapes, as shown in Fig. 8, must be checked and excluded during the optimisation. If two points on the stiffener are too close as shown in Fig. 8 (2), then there are probably highly distorted elements in this region. A stiffener with a small angle as shown in Figure 8 (3) can generate distorted elements as well and therefore must be excluded, too. All these three inadequate stiffener shapes are detected in the software by three user defined functions and respectively excluded automatically.

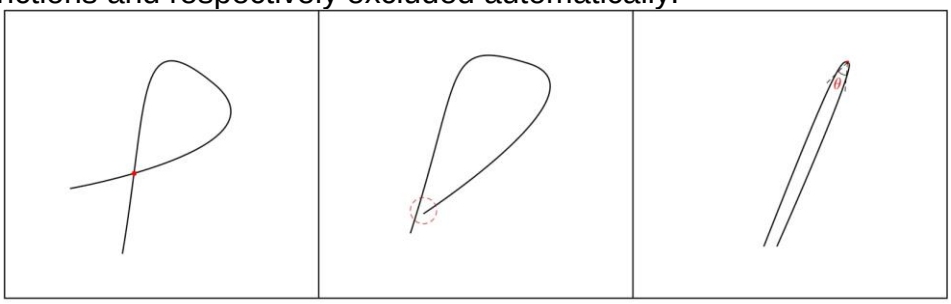

Figure 8: Unsuitable Stiffener Shapes

A new candidate of stiffener is resampled until it is acceptable for calculation in ABAQUS. Usually, the algorithm takes round about 10 times to find a suitable candidate of the stiffener. It rarely comes up for the algorithm to fall into a dead loop to look for stiffener. If that happens unfortunately, the optimisation must be restarted manually.

6. Reduce Sound Power Radiation at Resonances

The new method starts from the optimisation of sound power radiated at a single resonance

$$\min f = P_i (i = 1,2,..., \pi)$$

or three resonances together

$$\min f = \sum_{i=1}^{3} P_i (i = 1,2,3)$$

The cross section of the stiffener has been chosen with a constant profile. The mass can be constant or varying during the optimisation. Therefore, the total number of parameters under optimisation is 4+2n_m (for constant mass) or 4+3n_m (for varying mass) where n_m is the number of point masses.

6.1 Discussion of Result

If only the curved stiffener is employed to reduce the sound power, the optimisation result at a single resonance or three resonances is displayed in Table 1. $\max \Delta P$ indicates the maximal sound power reduction in dB. Δm means the overall mass increase after optimisation. The plus (+) symbol indicates increase while the negative symbol (-) indicates reduction. It is seen from Table 1 that a single stiffener can particularly reduce the sound power at a lower resonance ($i = 1,2,3$) and at relatively higher resonances ($i = 10$) as well. However, the overall mass increases only slightly (<5.0%). When the first three resonances are optimised all together, the power emission can be reduced by 62.7%, while the total mass increases slightly larger than 5.0%.

Table 1: esults of Optimisation using Stiffener (Plate + S) only

	$i = 1$	$i = 2$	$i = 10$	$i = 1,2,3$
$\max \Delta P$ (dB)	-3.85	-4.90	-12.4	-4.28
Δm (kg)	+1.05	+0.89	+0.80	+1.17
Δm (%)	+4.65	+3.94	+3.50	+5.17

The result of the optimisation is even better if an additional point mass is employed together with the stiffener (Plate + S + M1) as shown in Table 2. The $m1$ in the table means the mass of M1.

Table 2: Results of Optimisation using Stiffener and One Mass (Plate + S + M1)

	$i = 1$	$i = 2$	$i = 10$	$i = 1,2,3$
$\max \Delta P$ (dB)	-4.83	-5.70	-30.8	-4.61
$m1$ (kg)	0.5	0.5	0.2	0.2
Δm (kg)	+1.45	+1.74	+0.96	+1.22
Δm (%)	+6.40	+5.90	+4.22	+5.38

Compared with the result in Table 1, even a small constant mass can generate a better result, e.g., i =1, 2 or 10. However, the total mass increases only by less than 2%. Note, that the power at mode 10 is strongly reduced because the velocity of the surface has been severely reduced and its distribution is highly distorted as well. Therefore, the maximal power reduction of mode 10 given in the Table 2 only has the meaning in the sense of optimisation.

6.2 Influences on Other Modes

The optimisation of one mode influences of course the acoustic responses of other modes, which can obviously be seen in Fig. 9. Due to optimisation, the peak of mode 10 disappears after an additional point mass got mounted there. The level of sound power in $\Delta\omega'$ becomes particularly low. Below mode 10 all the eigenfrequencies are more or less have been moved higher. The pattern of power response below mode 10 is changed as well. Many power levels at resonances are reduced together with mode 10 (e.g. mode 4 and 8). Since the influences are true, when optimising other modes, they are, therefore, not repeated.

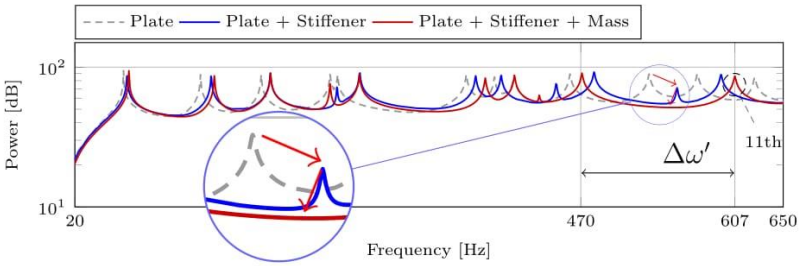

Figure 9: Optimisation Result for Mode 10

6.3 Effect of Mass

The effect of mass to reduce the power emission can be exemplified by the optimisation result of mode 2. As shown in Figure 10, the stiffener and mass do not modify the velocity pattern after optimisation. The optimal stiffener tries to embrace the two velocity modes, while the point masses maximally reduce the vibration by placing themselves at the two picks of the velocity modes. When the mass (m_1), in Fig. 9 (middle), is divided into two uniform masses (m_1, m_2), they are optimally located at the pick of the two velocity modes as shown in Fig. 9 (right). If the point mass is varying in range during the optimisation, its optimal value is close to the upper limit. It seems that a heavier mass at the velocity modes can optimally reduce the power radiation. This may be not true in the high frequency range, for the velocity distribution on surface is usually irregular after optimisation. For example, a single mass together with a stiffener particularly change the velocity distribution when the sound radiation at mode 10 is optimised. The velocity distribution is irregular and the optimal placement of the point mass cannot be expected.

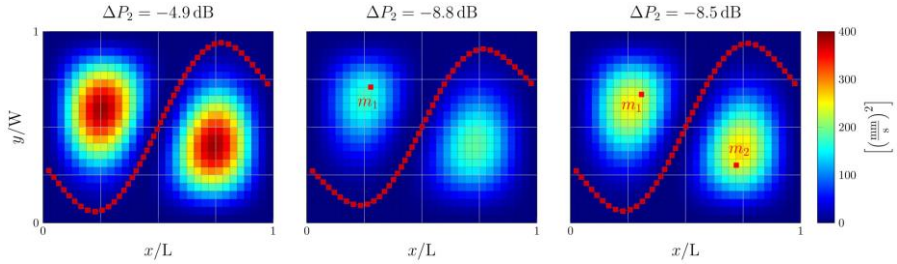

Figure 10: Optimisation Result of Mode 2

7. Reduce the Noise from Panels of a Railroad Freight Car

The optimisation method described before has been applied to a freight car to reduce the noise radiation from its panels. The whole procedure is shown in Fig. 11. The method of sub-model in ABAQUS has been employed to apply the optimisation methodology described with the panels. The whole freight car is defined as the global model and the selected panel is defined as a sub-model. The location of the excitation has been chosen that way that it can excite the whole structure under realistic conditions. The amplitude of the excitation comes from real on a railway track measured signals. The global model is analyzed only once while the sub-model is cyclically structural optimised. The frequency response of displacement along the boundaries of the sub-model is extracted from the global model and defined as the boundary condition during the optimisation process. It is assumed that the frequency response along the boundaries nearly does not change during the structural optimisation since the panel is much smaller in dimension compared to the whole wagon and the boundary is very stiff as well.

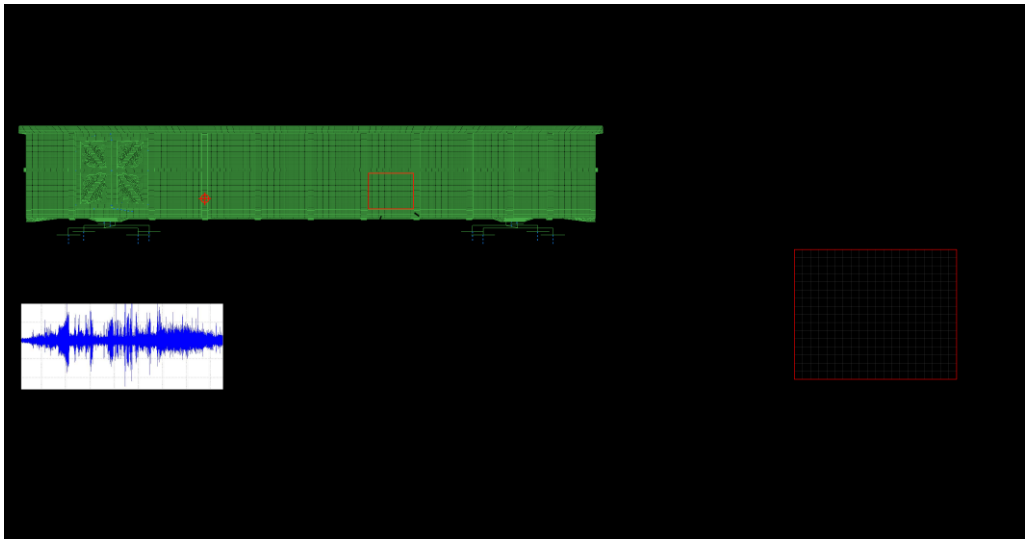

Figure 11: Reduction Process for the Calculation of the Power from the Panel

The optimisation frequency range ($\Delta\omega$) is selected to be from 175 Hz to 210 Hz, since the sound power level in this range before optimisation is relatively higher. The total power in this frequency range is then defined as

$$P_{\Delta\omega} = \int_{\Delta\omega} P(\omega) d\omega \tag{6}$$

where the unit of P is Watt. $P_{\Delta\omega}$ can be obtained by numerical integration. The frequency resolution is selected to be 1.0 Hz.
The power radiated from the panel is reduced by attaching a stiffener and one point mass of 200g (Plate + S + M1). After optimisation, the total sound power in $\Delta\omega$ is maximally reduced by nearly 2.8 dB. The optimisation result is displayed in Fig. 12.

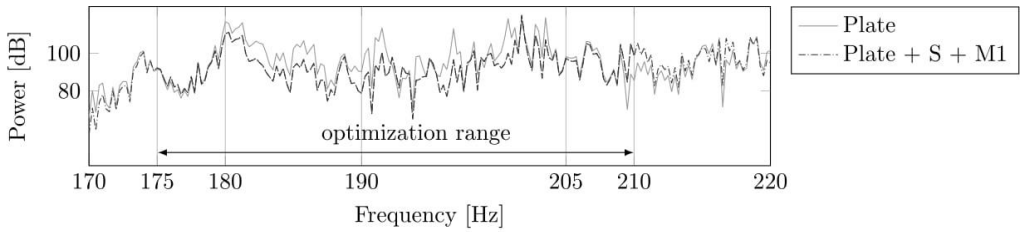

Figure 12: *Sound Power Reduction of Panel*

It can be seen from Fig. 11 that the level of power in $\Delta\omega$ is obviously reduced, while the power below and above the frequency limit does nearly not change. Thus, the primary purpose of this structural optimisation process was achieved.
The radiation efficiency (σ) in $\Delta\omega$ after optimisation is also reduced particularly as seen in Fig. 13, although the level is still very low. It seems that the reduction of efficiency in $\Delta\omega$ becomes smaller as the frequency goes higher.

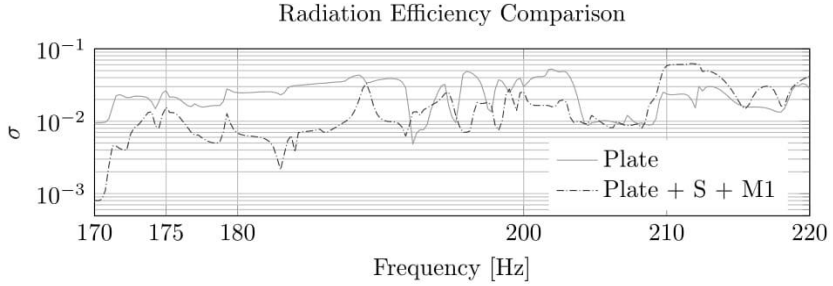

Figure 13: Radiation Efficiency after Optimisation

The total mass of the stiffener and the point mass increases only by 1.3 kg, which can be neglected compared to the whole wagon (22.6 t).

8. Conclusion

In this paper, a new method is presented to minimize the sound power radiated from panels by attaching a curvilinear stiffener and/or point masses. The well known global optimization method CMA-ES is employed to find the optimal stiffener shape and

placement of point masses. The method is firstly demonstrated to optimize the sound power radiated from a rectangular elastic plate. The results show that the new method is robust enough to reduce the sound power at a single resonance or three resonances together. The effect of reduction is even better when the point masses are attached together with the stiffener. However, the whole mass of model increases only slightly (<5.0%) after optimisation. The method is successfully extended to the panels of a freight car to reduce the sound radiation in a frequency band under complex boundary conditions (from the global model of the entire waggon). The results show that a curved stiffener with a single constant mass can particularly reduce the level of power and radiation efficiency in a given frequency band. The stiffener and point mass influences mainly the acoustic response in the given band while the responses out of the band are only slightly changed.
The new method is applicable to develop and design new structures with panel-like thin-walled areas, such as freight car, tank wagons or automobiles. As the attached components are made of steel or the same material as the surface, this method is also cost-effective. Since the new methodology is independent of frequency response, it is assumed, therefore, that it also works in the higher frequency range below 1000 Hz. However, it is more difficult to reduce the power as the modal density increases.

9. References

1 EUROPEAN COMMISSION (2014). “REPORT FROM THE COMMISSION TO THE EUROPEAN PARLIAMENT AND THE COUNCIL on the State of the Union Road Transport Market”.
2 Jr. St. Pierre, R. L. and G. H. Koopmann (1995). “A Design Method for Minimizing the Sound Power Radiated from Plates by Adding Optimally Sized, Discrete Masses”, J. Vib. Acoust. 117(B):243-251.
3 Andreas Rousounelos (2010). “Reduction of sound radiation from automotive-type panels”, Thesis, © Andreas Rousounelos.
[4] Arup Guha Niyogi Tirtha Banerjee (2013). “Active control of radiated sound from stiffened plates using IDE PFC actuators”, Int. J. Acoust. Vib. 18(3):109-116.
5 Masahiro Toyoda and Daiji Takahashi (2005). “Reduction of acoustic radiation by impedance control with a perforated absorber system”, Journal of Sound and Vibration. 286(3):601-614.
6 Alain Ratle and Alain Berry (1998). “Use of genetic algorithms for the vibroacoustic optimization of a plate carrying point-masses”, J. Acoust. Soc. Am. 104(6):3385-3397.
7 RL St Pierre and GH Koopmann (1995). “A design method for minimizing the sound power radiated from plates by adding optimally sized, discrete masses”, J. Mech. Des. 117(B):243-251.
8 Richard L. St. Jr. Pierre and Gary H. Koopmann (1993). “Minimization of radiated sound power from plates using distributed point masses”, The American Society of Mechanical Engineers, New York, NY.
9 A. D. Belegundu, R. R. Salagame, and G. H. Koopmann (1994). „A general optimization strategy for sound power minimization”, Struct. Optim. 8(2-3):113-119.
10 Nikolaus Hansen (2006). The CMA Evolution Strategy: “A Comparing Review. In Jose A. Lozano, Pedro Larrañaga, Iñaki Inza, and Endika Bengoetxea, editors, To-

wards a New Evolutionary Computation, number 192 in Studies in Fuzziness and Soft Computing", Springer Berlin Heidelberg. 75-102.
11 N. Hansen and A. Ostermeier (2001). «Completely derandomized self adaptation in evolution strategies", Evol Comput. 9(2),159-195.
12 Nikolaus Hansen (2005). "The CMA Evolution Strategy", A Tutorial.